Vietnam Journal of Science and Technology ***62*** *(6) (2024) 1210-1226*

doi:10.15625/2525-2518/19371

Aerofoil optimization using SLSQP and validation using numerical and analytical methods

Srinath R.[1, *], Mukesh R.[2], Inamul Hasan[3], Radha Krishnan P.[4]

[1]*Department of Aerospace Engineering, Dayananda Sagar University, Bangalore, India*

[2]*Department of Electronics and Communication Engineering, Saranathan College of Engineering, Tiruchirappalli, India*

[3]*Department of Aeronautical Engineering, Ramiah Institute of Technology, Bangalore, India*

[4]*Department of Aeronautical Engineering, ACS College of Engineering, Bangalore, India*

[*]Email: *srinathiyer9106@gmail.com*, *srinath.r@dsu.edu.in*

Received: 7 November 2023; Accepted for publication: 28 March 2024

Abstract. Aircraft design optimization is one among the research enriched topic in the aerospace industry, with enhancing aircraft performance, safety, and efficiency numerous being the prime focus areas. The work done demonstrates the application of the Sequential Least Squares Programming (SLSQP) technique over a symmetrical aerofoil "NACA 0012" to improve its aerodynamic performance. The optimized aerofoil is validated using Design and Analysis Tools for Composite Aircraft (DATCOM) and Computational Fluid Dynamics (CFD) methods. The results reveal, the optimized aerofoil has a significant reduction in drag coefficient of closer to 11 % between 8° and 10° compared to the initial design. The validation using DATCOM and CFD methods confirms the accuracy and usefulness of the optimization results. Validation error values are found to be negligible when compared to the optimization data, coming in at 5.7 % and 6.5 % for DATCOM and CFD, respectively. The paper highlights that the SLSQP technique is efficient and reliable optimization method for designing high-performance aerofoils.

Keywords: Optimization Technique, DATCOM, CFD, SLSQP technique.

Classification numbers: 5.4.4, 5.6.2, 3.4.5

1. INTRODUCTION

Since the 1970s, several techniques have been used to optimize aerofoil performance for particular applications on aircraft design. In recent years, multidisciplinary design optimization of aerofoils provides an integrated approach that interrelates various design parameters and disciplines. Inverse Design, based on gradient-based optimization and Numerical Optimization, based on direct search algorithms, are the two predominant optimization methods for designing aerofoils [1]. For instance, used a genetic algorithm approach to optimize the cavity of the aerofoil to increase the lift-to-drag ratio of a turbine blade, demonstrating significant improvements of a 31 % rise in Aerodynamic efficiency over the traditional aerofoil model [2]. Similarly Genetic algorithm and Bezier curve approach were employed to optimize the aerofoil

shape for a high lift, achieving superior performance [3]. Whereas the work on NACA 0012 aerofoil by [4] proved that the Machine learning-based optimization algorithm offered an optimized aerofoil in terms of enhanced aerodynamic properties. The outcomes of the obtained results are also validated. An aerodynamic shape optimization problem formulated for NACA 0012 aerofoil and solved using the methods of simulated annealing and genetic algorithm for a 5.0-degree angle of attack by [5] showed that the simulated annealing optimization scheme is more effective in finding the optimum solution among the various possible solutions. The weight of a UAV is reduced by optimizing the wing characteristics [6]. On a similar approach [7] employed high-fidelity computational codes, FLUENT and DIAMOND/IPSAP for the loose coupling Fluid Structure interaction optimization to enhance the endurance of UAV.

The parameterization method used for optimization must be able to model the aerodynamic body accurately. Also, it should be flexible enough to take all the possible shapes in the design space [8]. Various types of parameterization techniques are available to represent an aerofoil with the least number of parameters [9]. Bezier control points is used as a parameterization method to represent the aerofoil with the least number of parameters to increase the efficiency of an aerofoil (change in the momentum of flow) [10]. Classical and advanced parameterization methods in hands with optimization may solve many optimization problems. Aeroacoustics noise issues of a rotating wind turbine blade can essentially reduce by optimizing the NACA 0012 aerofoil using class/shape transformation [11]. The Bezier curve can be used to obtain the optimum locations of the Bezier control points that approximately represent the aerofoil shape (described using a set of data points) [12]. Ref. [8] presented the Bezier curve approximation of aerofoil using fourth-order, sixth-order and eighth-order Bezier curves and concluded that the sixth-order Bezier can accurately model the aerofoil shape

Optimization of aerofoils using the sequential least square programming (SLSQP) technique is an active area of research, with several studies showing promising results. For example, the SLSQP techniques is used in aerodynamic shape optimization (ASO), coupled with Topology optimization and claimed SLSQP as one of the most efficient optimization strategies [13]. The solution refinement is obtained for improving gas turbine performance through optimization using a gradient-based sequential least squares quadratic programming (SLSQP) algorithm [14]. Optimization method followed in the paper used the similar strategy used by [15] to optimize the RAE 2822 transonic type of aerofoil to improve its efficiency. A multi-variable design-constrained optimization of the conceptual BWB configuration uses the SLSQP algorithm [16].

The results obtained through optimization may or may not be accurate. Numerical validations and wind tunnel testing methods will be the optimal solution to check the results' accuracy. Two commonly used methods for validating optimization results are DATCOM and (CFD). The DATCOM, "Digital Datcom," is a popular tool for forecasting an aircraft's aerodynamic properties. The aerofoil data of existing NACA and other types of aerofoils are presented [17]. It uses a set of empirical formulas to compute the forces and moments acting on the aircraft under various flight conditions. The DATCOM provides accurate data for conventional aerodynamic shapes, and it is one of the classical validation methods, whereas the validation of unconventional shapes is not feasible [18]. The lift and drag characteristics of the aerofoil can be determined using DATCOM. The aerodynamic estimation (analytical) of lift and drag carried out on a three-dimensional UTM Elang-1 UAV using DATCOM [19] can also be an essential tool during the design phase of an aircraft. Ref. [20] expressed that during the optimization of a UAV, they used DATCOM and CFD as analytical tools to design the T-shaped stabilizer.

Whereas CFD is a numerical method used to simulate fluid flows and predict the aerodynamic performance of aircraft. It uses mathematical equations to model the airflow around the aircraft, considering factors such as turbulence, pressure, and viscosity. Simulations provide exhaustive information about the airflow and pressure distribution around the aircraft, making it a powerful tool for validating optimization results. The CFD analysis carried out on NACA 0012 aerofoil by [21] produced insightful results and are in good agreement with experimental results. The CFD results for transonic flow conditions over NACA 0012 aerofoil show that the predicted lift, drag and pressure coefficients are on par with the utmost accuracy with the experimental results [22]. The stability and control derivatives for the subsonic, low angle of attack (less than 15 degrees) flight regimes are predicted by the Digital DATCOM program due to its economic and time efficiency [23]. The DATCOM aerodynamic results were very close when compared to CFD. In this work, the NACA 0012 aerofoil is optimized using a Python-based optimizer SciPy which uses the SLSQP algorithm. The data obtained after the optimization procedure is validated using DATCOM and CFD.

2. METHODOLOGY

The objective of the methodology is carried out in two phases as Optimization and Validation optimizing the performance of an aerofoil follows as systematic approach as exposed in the Figure 1. A suitable baseline aerofoil profile NACA 0012 is selected based on the requirements and constraints relevant to the intended application. Key aerodynamic performance metrics are optimized, such as lift-to-drag ratio, lift coefficient, and drag coefficient. B-spline curves represent the aerofoil shape, providing flexibility and smoothness to describe the geometry accurately. The optimal number and strategic placement of control points are determined to capture the aerofoil's shape variation effectively.

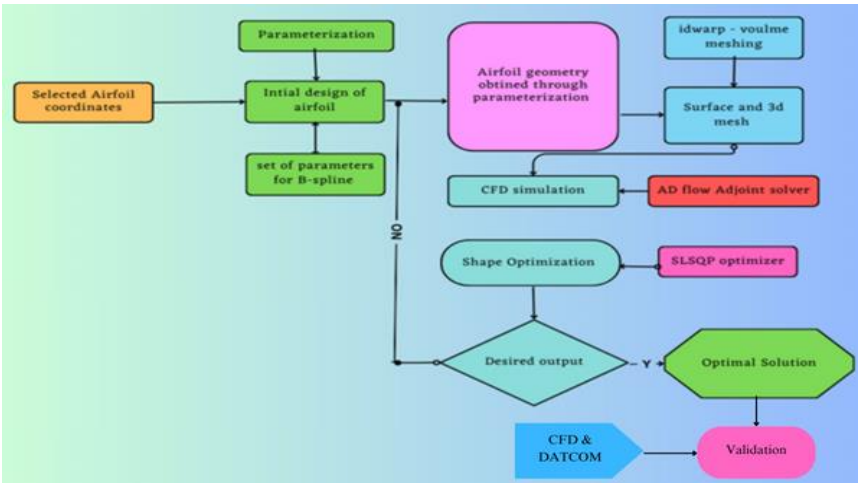

Figure 1. Methodology followed for optimization of aerofoils.

A high-quality surface mesh enhances the output efficiency after defining the aerofoil geometry using B-Spline curves. This surface mesh is extruded to create a 3D mesh suitable for numerical simulations. An ADflow adjoint solver is employed for sensitivity analysis and calculating the objective function's gradients concerning the control points. Next, the objective function describes the minimization or maximization problem based on the desired aerodynamic

performance metrics. Additionally, relevant constraints, such as maintaining minimum thickness at specific locations, are defined to be satisfied during the optimization process. The SLSQP optimizer, a gradient-based optimization algorithm, is implemented for shape optimization. Appropriate convergence criteria and constraints are set to ensure efficient and feasible Optimization.

Following the optimization process, the performance metrics of the optimized aerofoil are evaluated. If the desired output is achieved and the performance meets the requirements, optimization is concluded. However, an iterative approach is adopted if the optimization fails to meet the desired objectives or constraints. The B-Spline control points are updated, and the optimization process is repeated to explore new designs. By adhering to this systematic methodology, engineers and researchers can effectively optimize aerofoil designs using B-Spline parameterization and the SLSQP optimizer, ultimately leading to enhanced aerodynamic performance for specific applications. After obtaining the optimal solution the optimized aerofoil obtained goes through the validation phase (CFD and DATCOM analyses)

3. OPTIMIZATION PROBLEM

Symmetrical Aerofoil NACA 0012 was chosen to be optimized using open-source algorithms. Aerodynamic shape optimization of aerofoil follows a standardized procedure to obtain the optimal results, shown in Fig. 2. SLSQP is used to optimize the shape of aerofoils. Optimization techniques involve finding the optimal shape of an aerofoil that maximizes aerodynamic performance or minimizes drag while satisfying design constraints. Optimization involves defining the design variables, the objective function, and the design constraints and iteratively searching for the optimal solution using a gradient-based approach.

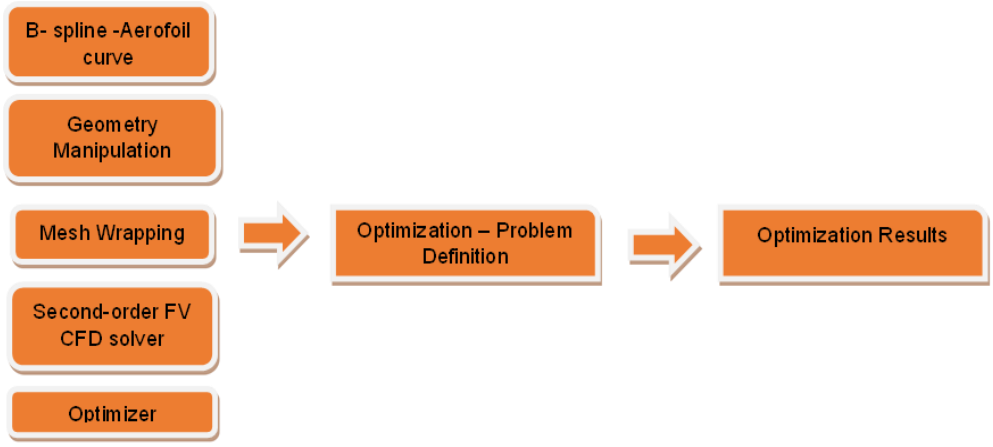

Figure 2. Standard procedure of optimization algorithm.

During the optimization of aerofoils, the algorithmic steps involved in using these techniques are as follows:

3.1. Define the design variables

The first step in optimizing an aerofoil is to define the design variables, which includes geometric parameters such as the shape of the aerofoil, the angle of attack, the thickness distribution, and the camber. Table 1 provides the input values of NACA 0012 aerofoil for optimization.

Table 1. Input values to define the aerofoil for optimization.

aExp	**3.0**
Alpha	0.25
bucket size	8
cornerAngle	30.0
errTol	0.0005
evalMode	'fast'
fileType	'CGNS'
gridFile	'n0012.cgns'

A parameterization technique defines the aerofoil shape with the least amount of data. The Bezier curve is the parameterization method employed here. The Bezier curve parameterization technique is used to obtain the aerofoil profile to improve the aerodynamic performance using a flow control device [10]. Bezier parameterization technique uses a spline curve which defines the NACA 0012 with 11 Bezier points, as shown in Table 2.

Table 2. Bezier Control Points.

X/C	Upper	Lower
-1.00E-03	0.020015	-0.02221
1.10E-01	0.06661	-0.06661
2.22E-01	0.074691	-0.07469
3.33E-01	0.0742	-0.0742
4.44E-01	0.068769	-0.06877
5.56E-01	0.059906	-0.05991
6.67E-01	0.048916	-0.04892
7.78E-01	0.035908	-0.03591
8.90E-01	0.021346	-0.02135
1.001e+00]	0.004985	-0.00534

Bezier curves are a preferred technique to achieve the desired aerofoil shape, as they are widely recognized for their representation of aerofoils. A Bezier curve is a parametric curve consisting of Bernstein basis polynomials generalized by the Equations 1 - 3. The use of 11 points is a general practise, but it's not a strict rule, with primary considerations for selecting 11 control points was computational efficiency. The NACA symmetric, asymmetric RAE and Eppler types of aerofoils are represented using six to fourteen control points [8, 12, 24]

$$P(u) = \sum_{i=o}^{n} PiBi, n(u) \; ; u \in [0, 1] \tag{1}$$

where n is the degree of the polynomial (defined by the control points), n = number of control points – 1, u is the parametric variable, Bi, n is Bases function; Bases functions are defined by the equation,

$$B_{i,\,n} = \frac{n!}{I!(n-i)!}\ UI\ (1 - u)^{n-i} \tag{2}$$

Formulas can generate the parameter equation of a curve defined by four control points (1) and (2) as a quadratic curve:

$$P\ (u) = P_0(1-u)^3 + 3P_1u(1-u)^2 + 3P_2u^2\ (1-u) + P_3u^3. \tag{3}$$

3.2. Define the objective function

The objective function is the performance metric that needs to be maximized or minimized. In the case of aerofoils, the objective function is typically the reduction of drag or to improvise the lift-to-drag ratio (aerodynamic efficiency). The objective function minimizing coefficient of drag (C_d): ($C_d < 0.063$)

3.3. Define the design constraints

Design constraints are defined to ensure that the optimal shape of the aerofoil satisfies specific requirements such as the maximum thickness, minimum camber, or the allowable angle of attack where Table 3 details the input values.

Table 3. Design Constraints.

Sl. No	Functions	Values
1.	Coefficient of lift (C_l)	≤ 0.6
2.	t/c at 30 %C	0.128
3.	t/c at 90 %C	6.5
4.	θ at LE	0.128
5.	θ at TE	0.094

3.4. Perform optimization

Using SLSQP, the optimization algorithm iteratively searches for the optimal solution that satisfies the design constraints and maximizes or minimizes the objective function. The optimization algorithm employs a gradient-based approach, which involves computing the gradient of the objective function concerning the design variables and using this information to update the design variables iteratively.

3.5. Governing equations and optimizer

The RANS governing equations are used in the aerofoil optimization to model the flow. The final differential form of the equation of Reynolds Averaged Navier–Stokes provided by Spalart and Allmaras is articulated as in Equations 4 and 5.

$$X(u) = \frac{\partial(P)}{\partial t} + \nabla.G^n - \nabla.G^v - B = 0\ in\ \Phi\ , t > 0, \tag{4}$$

The conservative variables are represented by the vector P given by density, velocity and energy $\{\rho, \rho v, \rho E\}$, respectively. Source term B and convective G^n and viscous fluxes $G^v$are well-defined by the equation

$$\boldsymbol{X}G^n = \begin{Bmatrix} \rho v \\ \rho vv + \dot{I}p \\ \rho Ev + \rho v \end{Bmatrix}. \tag{5}$$

4. OPTIMIZATION PROCEDURE

It is a gradient-based optimization algorithm that iteratively improves the design by searching for the optimal solution in the direction of the negative gradient of the objective function [25]. The algorithm uses quadratic programming to minimize a quadratic approximation of the objective function subject to linear equality and inequality constraints. SLSQP is particularly useful when the objective function is smooth and the design space is small. The basic equation for a generic SQP optimization algorithm [26] is

$$\text{Minimize } f(x)$$

$$\text{For } x \in Q^n$$

$$\text{Subject to } h(x) = 0$$

$$g(x) \leq 0$$

where f : $Q^n \rightarrow Q$ is the objective functional, the functions h : $Q^n \rightarrow Q^m$ and g : $Q^n \rightarrow Q^p$ describe the equality and inequality constraints.

It uses quadratic programming to minimize a quadratic approximation of the objective function, subject to linear equality and inequality constraints. These constraints are defined based on design requirements. During each iteration, SLSQP evaluates the current aerofoil shape, computes the gradients of the objective function for the design parameters (control points in the case of aerofoil shape parameterization using B-Spline curves), and then updates the design variables accordingly. The optimization continues until convergence, where the objective function or design variables change becomes negligible. By leveraging advanced algorithms and optimization techniques such as SLSQP, we have streamlined the optimization process, significantly reducing the computational time required for convergence [27].

The SLSQP optimizer uses the following steps to optimize the aerofoil [28]. Providing initial design variables to the SLSQP optimizer, the geometry of the aerofoil is defined by Bezier curve by pyGeo. Using high-fidelity CFD tools, the changed volume mesh is subjected to flow simulation; in this case, AD flow is employed while pyGeo computes geometric constraints The optimizer receives the total derivatives computed by the adjoint computation module in order to update the design variables. Rigorous set of iteration is performed. This iterative process ensures an optimized aerofoil design. RANS model was used as solver for a velocity of 40 m/s at the ground level altitude.

The optimum outcome, subject to constraints and satisfying the objective function, was obtained after 118 iterations. Multiple aerofoil shapes are explored during the optimization process as shown in Figure 3a, and their corresponding aerodynamic performance metrics are evaluated using CFD simulations. The Figures 3a and 3b show the comparative study of the various and optimized aerofoil shapes obtained. On the other hand, Figure 3c illustrates the base and optimised aerofoil's pressure coefficients.

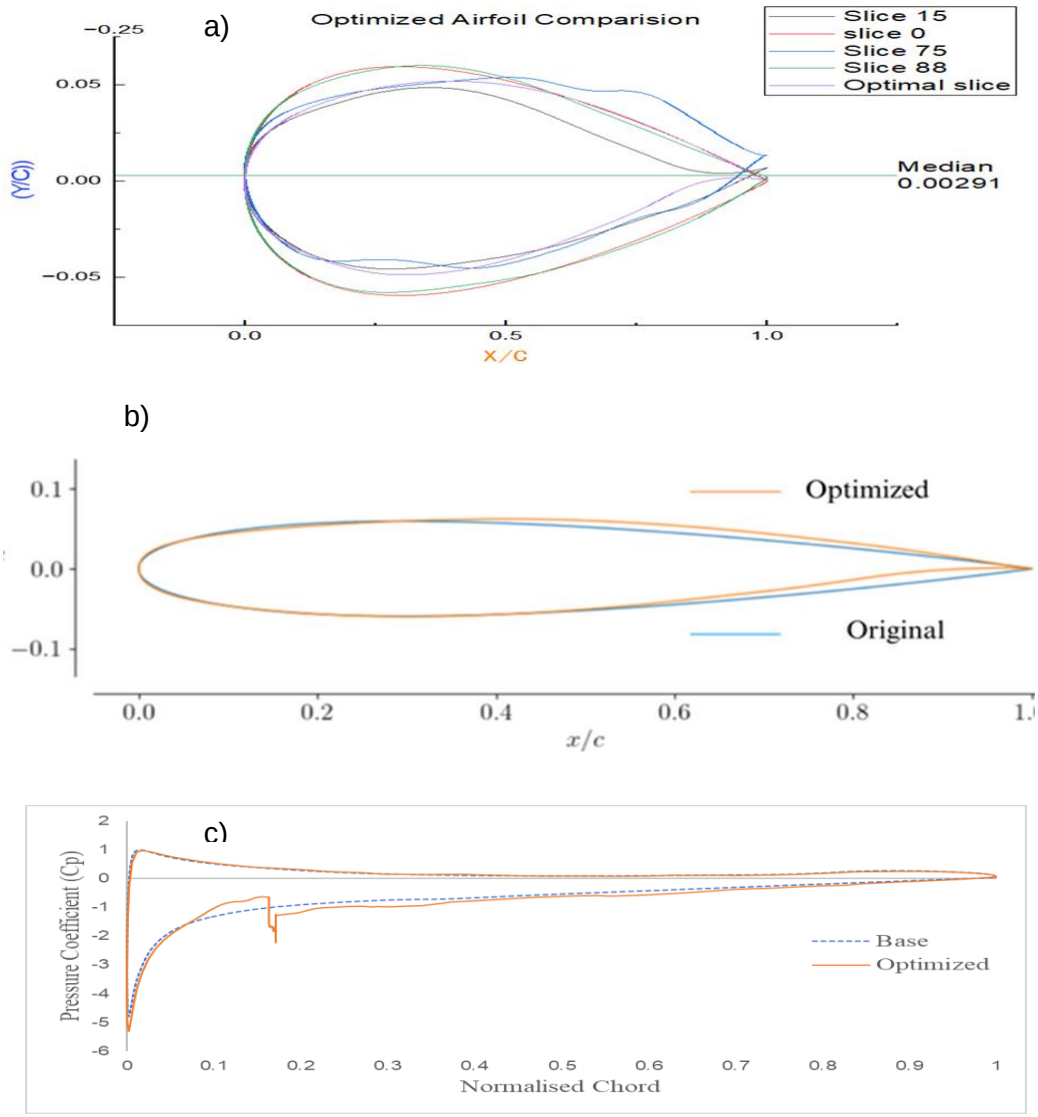

Figure 3. a) Aerofoil shapes obtained from SLSQP optimization algorithm *b)* Comparison between optimized and base line aerofoil *c)* Comparison of pressure coefficient between optimized and original aerofoils

5. VALIDATION OF OPTIMIZED DESIGN

5.1. Validation through DATCOM

DATCOM (Data Compendium) is a software program used in aerospace engineering to calculate the aerodynamic characteristics of aircraft, missiles, and other flying vehicles [30]. It was initially developed in the 1950s by the United States Air Force and has since been used extensively in the aerospace industry to design, analyze, and test aircraft and missile systems. The software is designed to calculate the aerodynamic characteristics of an aircraft or missile based on its geometry and operating conditions. The software considers various parameters such

as wing area, wing sweep, aspect ratio, and Mach number to calculate the vehicle's lift, drag, and moment coefficients. One of the critical features of DATCOM is its ability to handle a wide range of geometries and configurations. The software can handle both subsonic and supersonic flow regimes and can calculate the aerodynamic characteristics of configurations such as delta wings, swept wings, and canard configurations. The analysis of the optimized aerofoil at various angles of attack (-10° to +14°) is carried out at a Mach number of 0.6, considering the sea level altitude condition yielded the simulated values of coefficient of lift (C_l) and coefficient of drag (C_d) parameters. It is evident from Table 4 that the obtained values using software proved that the optimized aerofoil shows a decrease in drag near the stall angles.

Table 4. Force and moments of optimized aerofoil obtained through DATCOM software.

ALPHA	C_d	C_l	C_M	C_N	C_A	X_{CP}	CLA
-10	0.066	-1.62	-0.0656	-1.607	-0.216	0.041	1.75E-01
-8	0.05	-1.226	-0.0704	-1.221	-0.121	0.058	1.95E-01
-6	0.038	-0.839	-0.0751	-0.839	-0.05	0.09	1.91E-01
-4	0.031	-0.463	-0.0796	-0.464	-0.001	0.172	1.85E-01
-2	0.028	-0.1	-0.084	-0.101	0.025	0.83	1.79E-01
0	0.029	0.255	-0.0882	0.255	0.029	-0.346	1.81E-01
2	0.031	0.625	-0.0926	0.626	0.012	-0.148	1.89E-01
4	0.035	1.01	-0.0972	1.01	-0.028	-0.096	1.95E-01
6	0.042	1.405	-0.102	1.403	-0.091	-0.073	1.99E-01
8	0.052	1.606	-0.1069	1.799	-0.177	-0.059	1.96E-01
10	0.077	1.891	-0.1116	2.173	-0.284	-0.051	1.73E-01
12	0.098	1.905	-0.1155	2.469	-0.404	-0.047	1.40E-01
14	0.118	1.749	-0.1189	2.7	-0.532	-0.044	1.07E-01
16	0.152	1.625	-0.1214	2.854	-0.661	-0.043	7.01E-02

5.2. Validation through CFD

The numerical simulation of both the optimized and original aerofoil has been conducted using ANSYS CFD Fluent by solving the SPALART ALMARAZ equation over the defined boundary region of the aerofoil, in their analysis to simulate the flow over a supercritical aerofoil [31]. The SPALART ALMARAZ equation is specifically designed for aerospace applications involving wall-bounded flows, where the viscosity-affected region of the boundary layer needs to be properly resolved.

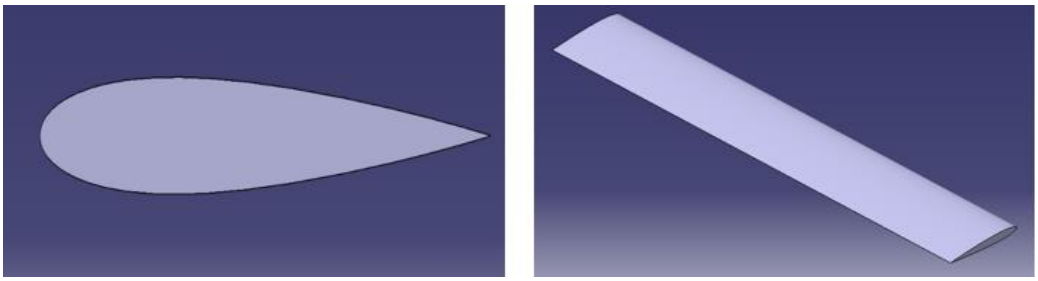

Figure 5. 2D and 3D design of non-optimized symmetric aerofoil.

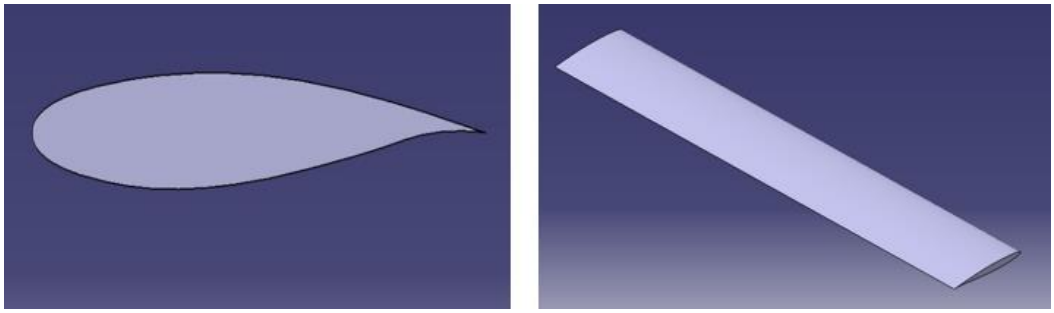

Figure 6. 2D and 3D design of optimized aerofoil.

The design of any model to be analyzed by CFD is carried out in a design software such as CATIA. The 2D and 3D designs of the base and optimized aerofoil, intended for subsequent simulations, are illustrated in Fig. 5 and Fig. 6. The 3D model, which possesses a chord length of 300 mm and a span of 550 mm, is also depicted in the figure. The coordinates of the optimized aerofoil are obtained post-optimization, while the base aerofoil coordinates are obtained from the NACA website UIUC aerofoil database.

The use of CFD analysis and the stages are detailed in forward analysis of supercritical aerofoil used in helicopters [32]. During pre-processing, the boundary condition required for simulation is fed as the input data, and the aerofoil is meshed [33]. Unstructured tetrahedral meshing is used to carry out the meshing for both aerofoils. Finer meshing with higher nodes is used closer to the trailing edge since they provide better results. The inlet velocity for the simulation is 35 m/s, where simulation is carried out for constant velocity at various angles of attack (AoA). The estimated wall distance from the boundary is 1.01 $E^{-5.}$ (Fig. 7), showing the cut section of mesh over the aerofoil and surface meshing created over a wing surface. Table 5 demonstrates the mesh property over the aerofoil section.

Table 5. Mesh properties of aerofoil.

Total no of elements	7204209
Total number of nodes	1823867
T grid skewness	In the range of 0.25-0.80
Prism layer for boundary layer interaction	15
Type of mesh	Unstructured Tetrahedral

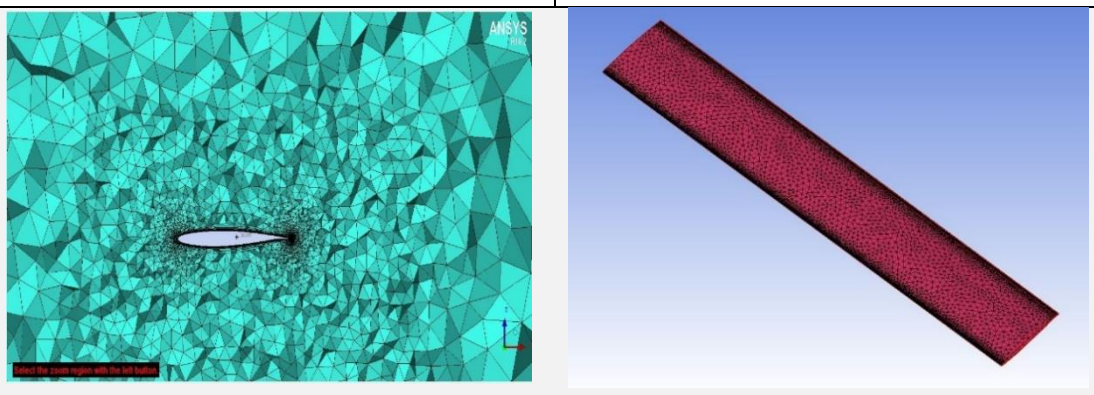

Figure 7. Meshing over optimized aerofoil section.

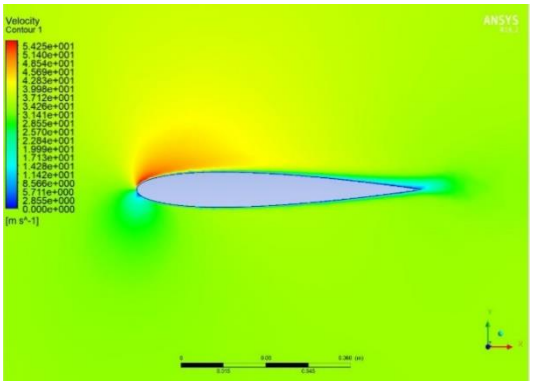

Figure 8. Velocity contour of non-optimized aerofoil @ 10° and 14° Angle of attack.

Whereas in the case of the optimized aerofoil, the flow separation area occurs at a higher angle when compared to non-optimized aerofoil; this is evident as the velocity over the optimized aerofoil is higher on the upper surface from the leading edge to mid chord line, which in turn reduces the flow separation or adverse pressure gradient. The comprehensive analysis of velocity contours at varying angles of attack (as depicted in Figures 9 and 10) has yielded valuable insights into the flow characteristics over the NACA 0012 aerofoil across diverse attack angles. The results can be used to optimize the design of aerofoils for improved performance in aerospace applications.

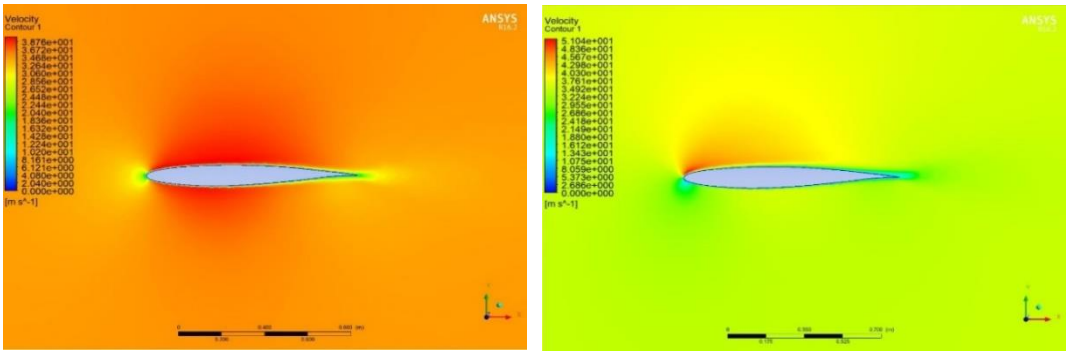

Figure 9. Velocity contour optimized aerofoil @ 0° and 8° angle of attack.

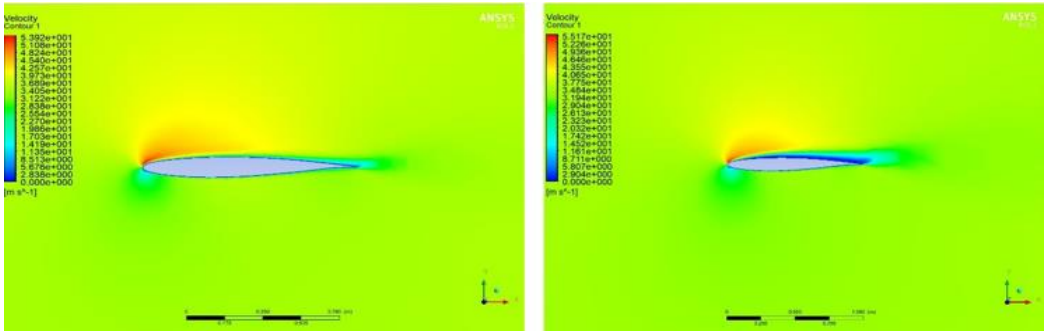

Figure 10. Velocity contour optimized aerofoil @ 10° and 14° angle of attack.

The stagnation point is located near the frontier portion of the aerofoil, but its location alters with a different angle of attack. Figure 11 illustrates that the point of stagnation coincides with the region of maximum pressure. As the airflow departs from the stagnation point and proceeds towards the trailing edge, there is a discernible reduction in pressure on the upper surface, particularly at higher angles of attack. As the flow is nearing the trailing edge, there is a slight increase in the pressure distribution due to the adverse pressure gradient. The flow velocity rises as it moves away from the front edge and reduces again as it reaches the trailing edge, a consequence of air divergence. It is remarkable that at higher angles of attack, the divergence of the airflow occurs at a more rapid rate compared to lower angles of attack. Figure 12 indicates the effect of the pressure gradient and the flow anomalies. Consequently, the divergence level shifts downstream relative to 10º and 14º AoA. In the case of an optimized aerofoil, the pressure difference created at a higher angle of attack provides a better insight into reducing drag.

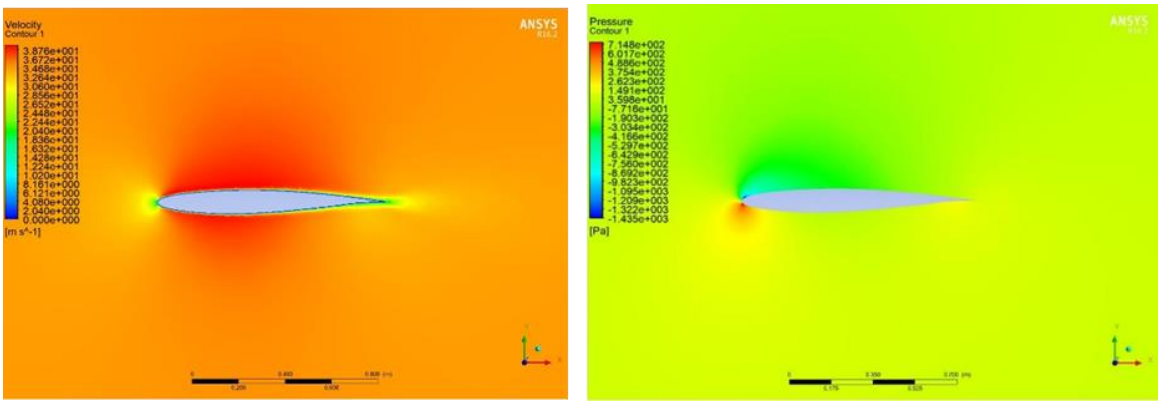

Figure 11. Pressure contour of NACA aerofoil @ 0° and 8° angle of attack.

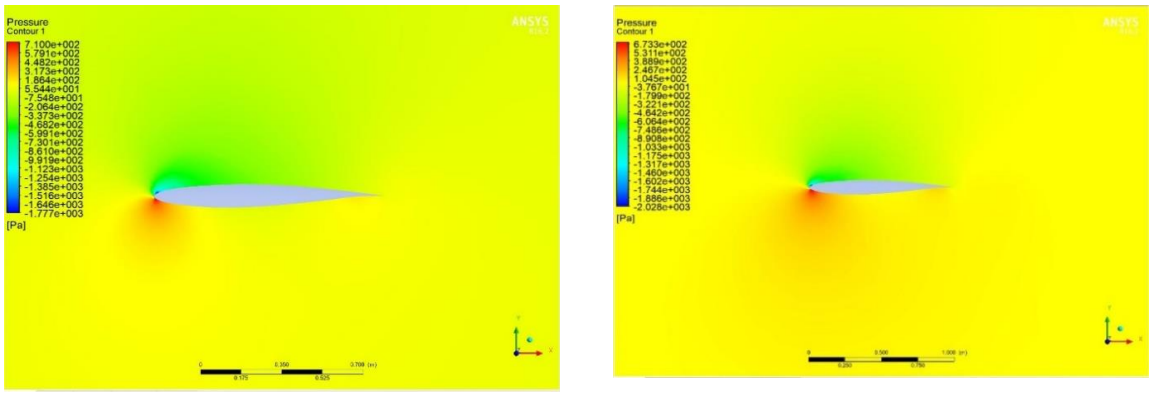

Figure 12. Pressure contour –NACA 0012 aerofoil @ 10° and 14° angle of attack.

The graphical representations of C_l and C_d values plotted against the angle of attack reveal distinct advantages of aerofoil optimization. Figure 13 expresses, at lower angles of attack, the optimized aerofoil exhibits lower C_d values than the non-optimized counterpart, indicating reduced drag. However, at higher angles of attack (beyond 10 degrees), the C_d values of the optimized aerofoil rise and approximate those of the non-optimized version.

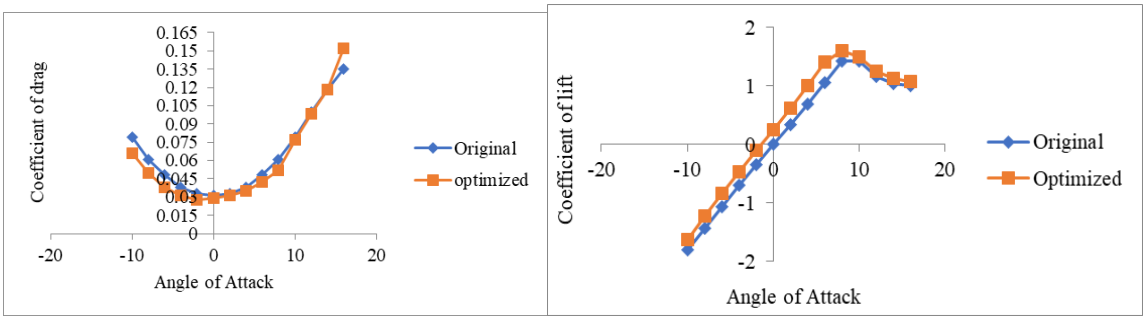

Figure13. Comparison of coefficient of drag and lift vs angle of attack for optimized and non-optimized aerofoil.

Unexpectedly, the optimized aerofoil demonstrates increased C_l values across all angles of attack, surpassing the performance of the non-optimized aerofoil as plotted in Fig. 13. These findings collectively emphasize the improved aerodynamic efficiency achieved through aerofoil optimization, characterized by lower drag at lower angles of attack and heightened lift generation across the entire angle of attack range.

6. RESULTS AND DISCUSSION

The comparative analysis of results achieved through CFD and the Digital Datacom tool (DATCOM) for both optimized and non-optimized aerofoils, executed across varying angles of attack, in Figure 14 and 15 distinctly illustrates a robust validation of the obtained data with the data set of positive angles of attack alone in case of optimized aerofoil. The acquired C_l and C_d values of the optimized aerofoil was meticulously compared with the outcomes derived from two different validation methods. Surprisingly, this comparative assessment reveals a negligible margin of error, providing further evidence of the accuracy and reliability of the results. Upon closer examination of the validation process, it becomes evident that the DATCOM tool plays a crucial role in enhancing the level of precision.

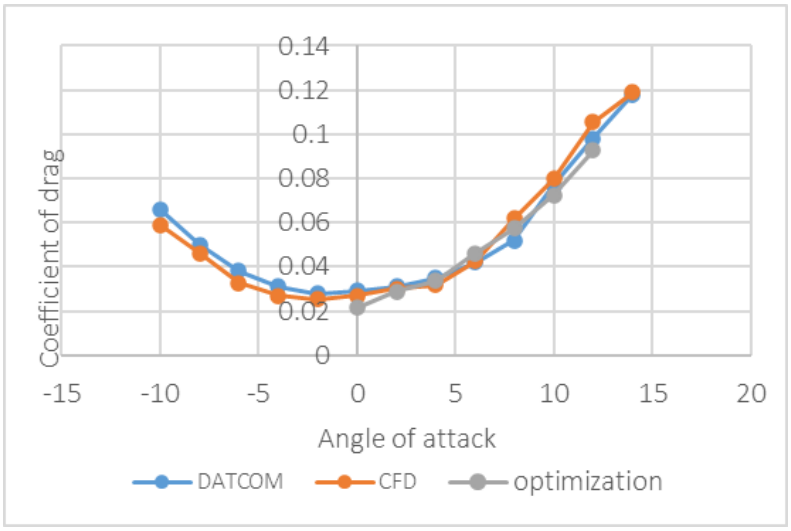

Figure 14. Comparative plots of Optimized aerofoil (C_d vs AoA)

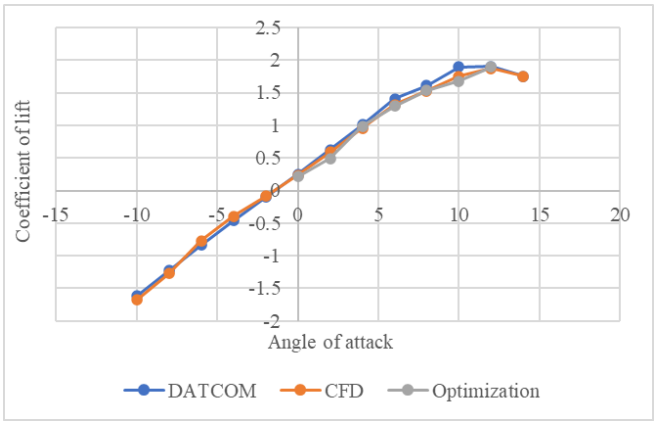

Figure 15. Comparative plots of Optimized aerofoil (C_l vs AoA).

7. CONCLUSION

The optimization of an aerodynamic profile increases overall efficiency. The goal of the work on the NACA 0012 aerofoil is to optimize the drag values by varying the body profile. Based on the requirements SLSQP and Bezier techniques are used as the optimization and parameterization algorithms, respectively. SPICY's SLSQP optimization techniques made a breakthrough in optimizing the profile, resulting in a decrease in drag coefficient with the given constraints. The computing time required for SLSQP approaches, which use Python code, is shorter when compared to other techniques used. In contrast to other approaches, the problem was solved within 118 iterations. Analyses were carried out to verify the outcomes. The values obtained following optimization are also validated twice by two traditional computational validation techniques. The reduction of 11.4 % in drag coefficient and a notable increase of 13.05 % in lift coefficient, is observed through a meticulous comparison between the optimized and original aerofoil data derived from DATCOM, lend robust support to the empirically established proposition that the optimized aerofoil excels over its non-optimized counterpart in the realm of aerodynamic efficiency. The convergence of minimal error rates of 5.7 % by DATCOM compared to an error percentage of 6.5 % from CFD collectively affirm the optimized aerofoil's pronounced superiority in aerodynamic performance, compared to the initial findings.

Acknowledgements. No funding by the agency and no conflicts of interest.

Credit authorship contribution statement. Dr. Srinath R- Conceptualization (lead), Data curation (lead), Formal analysis (equal), Investigation (lead), Validation (equal), Visualization (equal) Writing - original draft (equal). Dr. Mukesh R - Conceptualization (equal) Writing - original draft (equal), Writing - review & editing (equal). Dr. Inamul Hasan- Conceptualization (equal), Supervision (equal), Writing - original draft (equal), Writing - review & editing (equal). Dr. Radhakrishnan- Project administration (equal), Writing - original draft (equal).

Declaration of competing interest. The authors declare that they have no known competing financial interests or personal relationships that could have appeared to influence the work reported in this paper.

REFERENCES

1. Sharma P., Gupta B., Pandey M., Sharma A. K., and Nareliya Mishra R. - Recent advancements in optimization methods for wind turbine aerofoil design: A review, Materials Today: Proceedings, 2020. doi: 10.1016/j.matpr.(2021).02.231.

2. Fatehi M., Nili-Ahmadabadi M., Nematollahi O., Minaiean A., and Kim K. C. - Aerodynamic performance improvement of wind turbine blade by cavity shape optimization, Renew Energy **132** (2019) 773-785, doi: 10.1016/j.renene.2018.08.047.
3. Ayaz Ümütlü, H. C., and Kiral, Z. - Aerofoil shape optimization using Bezier curve and genetic algorithm, Aviation **26** (1) (2022) 32-40… doi: 10.3846/aviation.2022.16471.
4. Song X., Wang L., and Luo X. - Aerofoil optimization using a machine learning-based optimization algorithm, Journal of Physics: Conference Series (2022). doi: 10.1088/1742-6596/2217/1/012009.
5. Mukesh R., Lingadurai K., and Selvakumar U. -Application of nontraditional optimization techniques for aerofoil shape optimization, Modelling and Simulation in Engineering **2012** (2012). doi: 10.1155/2012/636135.
6. Yu J. - Design and Optimization of Wing Structure for a Fixed-Wing Unmanned Aerial Vehicle (UAV), Modern Mechanical Engineering **08** (04) (2018) 249-263, doi:10.4236/mme.2018.84017.
7. Son S. H., Choi B. L., Won W. J., Lee Y. G., Kim C. W., and Choi D. H. - Wing design optimization for a long-endurance UAV using FSI analysis and the kriging method, International Journal of Aeronautical and Space Sciences **17** (3) (2016). doi:10.5139/IJASS.2016.17.3.423.
8. Shikhar Jaiswal A. - Shape parameterization of aerofoil shapes using Bezier curves, Lecture Notes in Mechanical Engineering, **Part F9**, 2017, pp. 79-85. doi: 10.1007/978-981-10-1771-1_13.
9. Salunke N. P., Ahamad J. R. A., and Channiwala S. A. - Aerofoil Parameterization Techniques: A Review, American Journal of Mechanical Engineering **2** (4) (2014). doi:10.12691/ajme-2-4-1.
10. Srinath R., Mukesh R., Poojari M. C., Hasan I., and Amare Alebachew W. - Streamline Effect Improvement of Additive Manufactured Aerofoil Utilizing Dynamic Stream Control Procedure, Advances in Materials Science and Engineering **2022** (2022). doi:10.1155/2022/1252681.
11. Kou J., *et al.* - Aeroacoustic aerofoil shape optimization enhanced by autoencoders, Expert Syst Appl. **217** (2023). doi: 10.1016/j.eswa.2023.119513.
12. Agarwal D. and Sahu P. - A Unified Approach for Aerofoil Parameterization Using Bezier Curves, Comput. Aided. Des. Appl. **19** (6) (2022). doi: 10.14733/cadaps.2022.1130-1142.
13. Gibert Martínez I., Afonso F., Rodrigues S., and Lau F. - A Sequential Approach for Aerodynamic Shape Optimization with Topology Optimization of Aerofoils, Mathematical and Computational Applications **26** (2) (2021). doi:10.3390/mca26020034.
14. Storti B., Garelli L., Storti M., and D'Elía J. - Optimization of an internal blade cooling passage configuration using a Chimera approach and parallel computing, Finite Elements in Analysis and Design **177** (2020). doi: 10.1016/j.finel.2020.103423.
15. Kumar D., Raisee M., and Lacor C. - Combination of polynomial chaos with adjoint formulations for optimization under uncertainties, In: Notes on Numerical Fluid Mechanics and Multidisciplinary Design **140** (2019). doi:10.1007/978-3-319-77767-2_35.
16. Kleemann N., Karpuk S., and Elham A. - Conceptual design and optimization of a solar-electric blended wing body aircraft for general aviation, In: *AIAA* Scitech 2020 Forum, 2020. doi: 10.2514/6.2020-0008.

17. Dadone L. U. - US Army Helicopter Design DATCOM Volume I - Aerofoils, Datcom, Vol. I, September, 1976.
18. Gili P., Visone M., Lerro A., De Vivo F., and Scognamiglio G. - A new approach for the estimation of longitudinal damping derivatives: CFD validation on NACA 0012', WSEAS Transactions on Fluid Mechanics**, V**ol. 10, 2015.
19. Israr H. A. and Dahalan Md. N. - Estimation of Lift and Drag Characteristics of UTM Elang-1 UAV, 2nd Regional Conference on Vehicle Engineering and Technology 2008, no. October, 2008.
20. Popović L., Paunović L., Đilas V., Milutinović A., Ivanov T., and Kostić I. - Design of the UAV aerodynamics in multiple stages, Scientific Technical Review **70** (2) (2020). doi:10.5937/str2002009p.
21. Chumbre V., Rushikesh T., Umatar S., and Kerur S. M. - CFD Analysis of Aerofoil Sections, International Research Journal of Engineering and Technology (IRJET) **5** (7) (2018).
22. El Maani R., Radi B., and El Hami A. - CFD Analysis of the Transonic Flow over a NACA 0012 Aerofoil, Incertitudes et fiabilité des systèmes multiphysiques **2** (2) (2018) doi: 10.21494/iste.op.2018.0307.
23. Comparative cfd analysis of aerofoils for unmanned aerial vehicles, Int. J. Res. Eng. Technol **6** (5) (2017). doi: 10.15623/ijret.2017.0605005.
24. Wei X., Wang X., and Chen S. - Research on parameterization and optimization procedure of low-Reynolds-number aerofoils based on genetic algorithm and Bezier curve, Advances in Engineering Software **149** (2020). doi: 10.1016/j.advengsoft.2020.102864.
25. Kumar D., Miranda J., Raisee M., and Lacor C. - Adjoint based multi-objective shape optimization of a transonic aerofoil under uncertainties, in 5th International Conference on Engineering Optimization, 2016.
26. Hoppe R. W. - Chapter 4 Sequential Quadratic Programming, in Book, Chapter, 2006.
27. Marques J. P. P. G., Cunha D. C., Harada L. M. F., Silva L. N., and Silva I. D. - A cost-effective trilateration-based radio localization algorithm using machine learning and sequential least-square programming optimization, Comput Commun **177** (2021) doi:10.1016/j.comcom.2021.06.005.
28. Nagawkar J., Ren J., Du X., Leifsson L., and Koziel S. - Single- and Multipoint Aerodynamic Shape Optimization Using Multifidelity Models and Manifold Mapping, J. Aircr **58** (3) (2021). doi: 10.2514/1.c035297.
29. Hasan I., Mukesh R., Radha Krishnan P., Srinath R., Babu D. P., and Lemma Gurmu N. Wind Tunnel Testing and Validation of Helicopter Rotor Blades Using Additive Manufacturing, Advances in Materials Science and Engineering **2022** (2022). doi:10.1155/2022/4052208.
30. United States Air Force - The USAF Stability And Control Digital Datcom Volume 1: Users Manual, Technical Report, **Vol. I**, no. Apr 1979, 1979.
31. Hasan I., Mukesh R., Radha Krishnan P., and Srinath R. - Aerodynamic performance analysis of a supercritical aerofoil in the helicopter main rotor, Transactions of the Canadian Society for Mechanical Engineering**. 46** (2) (2022). doi:10.1139/tcsme-2021-0067.

32. Hasan I., Mukesh R., Radha Krishnan P., Srinath R., and Dhanya Prakash R. B. - Forward Flight Performance Analysis of Supercritical Aerofoil in Helicopter Main Rotor, Intelligent Automation and Soft Computing **33** (1) (2022). doi:10.32604/iasc.2022.023252.
33. Srinath R., R. Mukesh I. Hasan, and Krishnan P. R. - CFD Investigation of Dual Synthetic Jets on an Optimized Aerofoil's Trailing Edge, Journal of Applied Fluid Mechanics **17** (11) (2024). doi.org/10.47176/jafm.17.11.2709.